

Focusing light through scattering media by transmission matrix inversion

JIAN XU,* HAOWEN RUAN, YAN LIU, HAOJIANG ZHOU, AND CHANGHUEI YANG

Department of Electrical Engineering, California Institute of Technology, Pasadena, CA 91125, USA

*jxxu@caltech.edu

Abstract: Focusing light through scattering media has broad applications in optical imaging, manipulation and therapy. The contrast of the focus can be quantified by peak-to-background intensity ratio (PBR). Here, we theoretically and numerically show that by using a transmission matrix inversion method to achieve focusing, within a limited field of view and under a low noise condition in transmission matrix measurements, the PBR of the focus can be higher than that achieved by conventional methods such as optical phase conjugation or feedback-based wavefront shaping. Experimentally, using a phase-modulation spatial light modulator, we increase the PBR by 66% over that achieved by conventional methods based on phase conjugation. In addition, we demonstrate that, within a limited field of view and under a low noise condition in transmission matrix measurements, our matrix inversion method enables light focusing to multiple foci with greater fidelity than those of conventional methods.

© 2017 Optical Society of America

OCIS codes: (290.7050) Turbid media; (220.1080) Active or adaptive optics; (090.1995) Digital holography; (070.5040) Phase conjugation.

References and links

1. N. Ji, D. E. Milkie, and E. Betzig, "Adaptive optics via pupil segmentation for high-resolution imaging in biological tissues," *Nat. Methods* **7**(2), 141–147 (2010).
2. X. Xu, H. Liu, and L. V. Wang, "Time-reversed ultrasonically encoded optical focusing into scattering media," *Nat. Photonics* **5**(3), 154–157 (2011).
3. Y. M. Wang, B. Judkewitz, C. A. Dimarzio, and C. Yang, "Deep-tissue focal fluorescence imaging with digitally time-reversed ultrasound-encoded light," *Nat. Commun.* **3**, 928 (2012).
4. K. Si, R. Fiolka, and M. Cui, "Fluorescence imaging beyond the ballistic regime by ultrasound pulse guided digital phase conjugation," *Nat. Photonics* **6**(10), 657–661 (2012).
5. E. H. Zhou, H. Ruan, C. Yang, and B. Judkewitz, "Focusing on moving targets through scattering samples," *Optica* **1**(4), 227–232 (2014).
6. H. Ruan, J. Brake, J. E. Robinson, M. Jang, C. Xiao, C. Zhou, V. Gradinaru, and C. Yang, "Optogenetic Control of Neural Activity with Time-Reversed Ultrasound Encoded Light," in *Optics in the Life Sciences Congress* (2017), p. BrM3B.3.
7. J. Yoon, M. Lee, K. Lee, N. Kim, J. M. Kim, J. Park, H. Yu, C. Choi, W. D. Heo, and Y. Park, "Optogenetic control of cell signaling pathway through scattering skull using wavefront shaping," *Sci. Rep.* **5**, 13289 (2015).
8. Z. Huang, "A review of progress in clinical photodynamic therapy," *Technol. Cancer Res. Treat.* **4**(3), 283–293 (2005).
9. I. M. Vellekoop and A. P. Mosk, "Focusing coherent light through opaque strongly scattering media," *Opt. Lett.* **32**(16), 2309–2311 (2007).
10. I. M. Vellekoop and A. P. Mosk, "Universal optimal transmission of light through disordered materials," *Phys. Rev. Lett.* **101**(12), 120601 (2008).
11. Z. Yaqoob, D. Psaltis, M. S. Feld, and C. Yang, "Optical phase conjugation for turbidity suppression in biological samples," *Nat. Photonics* **2**(2), 110–115 (2008).
12. M. Cui and C. Yang, "Implementation of a digital optical phase conjugation system and its application to study the robustness of turbidity suppression by phase conjugation," *Opt. Express* **18**(4), 3444–3455 (2010).
13. C.-L. Hsieh, Y. Pu, R. Grange, G. Laporte, and D. Psaltis, "Imaging through turbid layers by scanning the phase conjugated second harmonic radiation from a nanoparticle," *Opt. Express* **18**(20), 20723–20731 (2010).
14. Y. Shen, Y. Liu, C. Ma, and L. V. Wang, "Focusing light through biological tissue and tissue-mimicking phantoms up to 9.6 cm in thickness with digital optical phase conjugation," *J. Biomed. Opt.* **21**(8), 85001 (2016).

15. S. M. Popoff, G. Lerosey, R. Carminati, M. Fink, A. C. Boccarda, and S. Gigan, "Measuring the transmission matrix in optics: An approach to the study and control of light propagation in disordered media," *Phys. Rev. Lett.* **104**(10), 100601 (2010).
16. A. Drémeau, A. Liutkus, D. Martina, O. Katz, C. Schülke, F. Krzakala, S. Gigan, and L. Daudet, "Reference-less measurement of the transmission matrix of a highly scattering material using a DMD and phase retrieval techniques," *Opt. Express* **23**(9), 11898–11911 (2015).
17. J. Yoon, K. Lee, J. Park, and Y. Park, "Measuring optical transmission matrices by wavefront shaping," *Opt. Express* **23**(8), 10158–10167 (2015).
18. M. Kim, W. Choi, Y. Choi, C. Yoon, and W. Choi, "Transmission matrix of a scattering medium and its applications in biophotonics," *Opt. Express* **23**(10), 12648–12668 (2015).
19. R. Horstmeyer, H. Ruan, and C. Yang, "Guidestar-assisted wavefront-shaping methods for focusing light into biological tissue," *Nat. Photonics* **9**, 563–571 (2015).
20. S. Popoff, G. Lerosey, M. Fink, A. C. Boccarda, and S. Gigan, "Image transmission through an opaque material," *Nat. Commun.* **1**, 81 (2010).
21. J. W. Goodman, *Statistical Optics* (Wiley, New York, 1985).
22. N. Garcia and A. Z. Genack, "Crossover to strong intensity correlation for microwave radiation in random media," *Phys. Rev. Lett.* **63**(16), 1678–1681 (1989).
23. J. B. Pendry, A. MacKinnon, and P. J. Roberts, "Universality Classes and Fluctuations in Disordered Systems," *Proc. R. Soc. A Math. Phys. Eng. Sci.* **437**, 67–83 (1992).
24. H. H. Barrett and K. J. Myers, *Foundations of Image Science / Harrison H. Barrett, Kyle J. Myers* (2004).
25. T. Zhang and I. Yamaguchi, "Three-dimensional microscopy with phase-shifting digital holography," *Opt. Lett.* **23**(15), 1221–1223 (1998).
26. G. H. Golub and C. F. Van Loan, *Matrix Computations* (Johns Hopkins, 2013).
27. A. M. Tulino and S. Verdú, "Random Matrix Theory and Wireless Communications," *Found. TrendsTM Commun. Inf. Theory* **1**, 1–182 (2004).

1. Introduction

Focusing light through scattering media has broad applications in areas such as biomedical imaging [1–4], cell cytometry [5], optogenetics [6,7] and photodynamic therapy [8]. However, because of the refractive index inhomogeneity, light is scattered when propagating through scattering media. To focus light through such turbid media, researchers have developed a number of wavefront shaping techniques, including feedback-based methods [9,10], optical phase conjugation [11–14] and transmission matrix methods [15–18]. Feedback-based methods employ a spatial light modulator (SLM) to continuously shape the wavefront of the incident light while monitoring the feedback signal from a guidestar which is proportional to the light intensity at a target location. In this way, an optimum wavefront can be obtained to maximize the light intensity at the target location to form an optical focus. Optical phase conjugation methods achieve light focusing by phase conjugating the scattering light field emitted from a guidestar [19] located at the target location. Traditionally, transmission matrix methods first measure the scattered light fields corresponding to different incident light fields (i.e. measure the transmission matrix), and then realize focusing by sending an appropriate incident field which is proportional to the linear combination of the columns of the transpose conjugation of the measured transmission matrix.

To focus light through scattering media, wavefront shaping methods typically use an SLM to increase the light intensity at the target location. This strategy is fundamentally tied to the concept of phase conjugation, i.e. using the finite elements of the SLM to align the phase of the incident wavefront to increase the intensity at the target location. Typically, the number of optical modes of the scattered light field is larger than the number of controllable elements on the SLM. Therefore, one can only partially conjugate the correct wavefront solution, which leads to a non-zero background surround the focus. The contrast of the focus can be quantified by a peak-to-background ratio (PBR), which is the ratio between the intensity of the focus and the average intensity of the background surrounding the focus. We note that our definition of PBR is different from the conventional wavefront shaping definition of PBR, which is the ratio between the focus intensity and the average intensity before wavefront shaping [9]. We chose to use our definition, since in most applications such as point-scanning microscopy and photolithography, the contrast of a focus in a single light pattern is an important parameter. In theory, the PBR of the focus is proportional to the number of degrees

of freedom (pixels or super-pixels) of the SLM [9]. This conclusion is intuitive because we can only increase the intensity at the target location by a limited amount, given that we have only a limited number of degrees of freedom. However, in a noise-free or very low noise situation, if we take the strategy to increase the intensity at the target location while darkening the background near the target location, we can achieve a focus with a higher PBR than that achieved by conventional methods in a given field of view (FOV). We will refer to this method as transmission matrix inversion, because mathematically it takes the pseudoinverse of the transmission matrix to realize it. Popoff et al. have demonstrated that using the inverse of the transmission matrix one can recover an image through scattering media with greater fidelity than that using the phase conjugation method [20]. The method we demonstrate here shares the same theoretical foundation with the transmission matrix inversion method they reported in ref [20]. In this work, we compare the transmission matrix inversion method and the phase conjugation method based on the optical focus (foci) directly measured (without reconstruction) after transmission through the scattering medium and find that the transmission matrix inversion method is able to focus light with higher contrast and fidelity under a noise-free or low noise condition. This high contrast light focus (foci) formed directly after transmission through scattering media has a number of important applications including point-scanning microscopy and photolithography.

2. Principle and simulation

Mathematically, we use a transmission matrix \mathbf{T} to relate the optical fields before (\mathbf{E}_{in}) and after (\mathbf{E}_{out}) transmitting through a scattering medium:

$$\mathbf{E}_{\text{out}} = \begin{bmatrix} E_{\text{out},1} \\ E_{\text{out},2} \\ \dots \\ E_{\text{out},m} \end{bmatrix} = \begin{bmatrix} t_{11} & t_{12} & \dots & \dots & \dots & t_{1n} \\ \dots & \dots & \dots & \dots & \dots & \dots \\ t_{m1} & t_{m2} & \dots & \dots & \dots & t_{mn} \end{bmatrix}_{m \times n} \begin{bmatrix} E_{\text{in},1} \\ E_{\text{in},2} \\ \dots \\ E_{\text{in},n} \end{bmatrix} = \mathbf{T}\mathbf{E}_{\text{in}}, \quad m < n. \quad (1)$$

Here, the scattering medium is described by a transmission matrix \mathbf{T} , whose elements t_{ij} follow a complex Gaussian distribution [21–23] with a zero mean and a variance σ^2 , i.e. $t_{ij} \sim CN(0, \sigma^2)$. The incident field \mathbf{E}_{in} is described by an $n \times 1$ vector and the output field \mathbf{E}_{out} is described by an $m \times 1$ vector. Here, m means that there are m modes in our interested FOV but does not mean that the total number of output optical modes is m after light propagates through the scattering medium. We assume $m < n$, which is the condition for theoretically realizing a zero background, as will be discussed in Section 2.1.

2.1 Focusing light to one target location

To focus light through scattering media by conventional methods such as phase conjugation, we obtain the appropriate incident light field by $\mathbf{E}_{\text{in}}^{\text{conj}} = \mathbf{T}^* \times \mathbf{E}_{\text{out}}$ [15]. Here, \mathbf{T}^* denotes the conjugate transpose of \mathbf{T} . If we want to focus light to one target location, without losing generality, we can set the desired output field $\mathbf{E}_{\text{out}} = [1 \ 0 \ \dots \ 0]^T$, where $[-]^T$ denotes matrix transpose. Thus, $\mathbf{E}_{\text{in}}^{\text{conj}}$ is the first column of \mathbf{T}^* , i.e. $\mathbf{E}_{\text{in}}^{\text{conj}} = \mathbf{T}^* \times [1 \ 0 \ \dots \ 0]^T$, and the output field achieved by the phase conjugation method can be calculated by

$$\mathbf{E}_{\text{out}}^{\text{conj}} = \mathbf{T} \times \mathbf{T}^* \times \begin{bmatrix} 1 \\ 0 \\ \dots \\ 0 \end{bmatrix}. \quad (2)$$

Because of the statistical property of the elements of \mathbf{T} , $\mathbf{T} \times \mathbf{T}^* \approx \alpha \mathbf{I}$, where \mathbf{I} is an identity matrix, α is a normalization coefficient. The intensity of the output field $\mathbf{I}_{\text{out}}^{\text{conj}}$ can be written as

$$\mathbf{I}_{\text{out}}^{\text{conj}} = |\mathbf{E}_{\text{out}}^{\text{conj}}|^2 = \begin{bmatrix} |E_{\text{out},1}^{\text{conj}}|^2 \\ |E_{\text{out},2}^{\text{conj}}|^2 \\ \dots \\ |E_{\text{out},m}^{\text{conj}}|^2 \end{bmatrix} = \begin{bmatrix} I_{\text{out},1}^{\text{conj}} \\ I_{\text{out},2}^{\text{conj}} \\ \dots \\ I_{\text{out},m}^{\text{conj}} \end{bmatrix} \approx \alpha^2 \begin{bmatrix} 1 \\ n^{-1} \\ \dots \\ n^{-1} \end{bmatrix}. \quad (3)$$

Since the elements t_{ij} of \mathbf{T} follow the complex Gaussian distribution, the probability theory shows that the expected value of $I_{\text{out},1}^{\text{conj}}$ (peak intensity) is n times higher than that of $I_{\text{out},k}^{\text{conj}}$ ($k \neq 1$, background intensity) [9]. Therefore, the PBR is limited by the number of independent incident optical modes n , which depends on the pixel number of the SLM. In this case, we use all the degrees of freedom to enhance only one specific output mode while doing nothing about the background (the rest of the modes). Moreover, the theory only predicts the intensity enhancement statistically based on the distribution of the elements of \mathbf{T} , the exact enhancement should be measured experimentally, or calculated based on the known transmission matrix \mathbf{T} .

However, if we take the matrix inversion, the enhancement is no longer limited by the pixel number on the SLM. Here, we choose the first column of the pseudoinverse of \mathbf{T} as the input field $\mathbf{E}_{\text{in}}^{\text{inv}}$, i.e. $\mathbf{E}_{\text{in}}^{\text{inv}} = \mathbf{T}^+ \times [1 \ 0 \ \dots \ 0]^T$, where $\mathbf{T}^+ = \mathbf{T}^* (\mathbf{T}\mathbf{T}^*)^{-1}$ denotes the Moore–Penrose pseudoinverse [24] of \mathbf{T} and it has the property of $\mathbf{T} \times \mathbf{T}^+ = \mathbf{I}$. Then, the output light field can be calculated by

$$\mathbf{E}_{\text{out}}^{\text{inv}} = \mathbf{T} \times \mathbf{E}_{\text{in}}^{\text{inv}} = \mathbf{T} \times \mathbf{T}^+ \times \begin{bmatrix} 1 \\ 0 \\ \dots \\ 0 \end{bmatrix} = \begin{bmatrix} 1 \\ 0 \\ \dots \\ 0 \end{bmatrix}. \quad (4)$$

Here, the Moore–Penrose pseudoinverse requires the condition of $m < n$ as mentioned in Section 2. The result in Eq. (4) shows that theoretically the background can be suppressed down to zero, thus the PBR can be increased to infinity. We should note that the phase conjugation is a special case of the Moore–Penrose pseudoinverse. When there is only one output mode (i.e. the transmission matrix is 1 by n), \mathbf{T}^* is the same as \mathbf{T}^+ except by a normalization factor. When there are more than one output modes, the transmission matrix inversion method not only increases the intensity of the focus, but also allocates some degrees of freedom to suppress the background intensity.

Figure 1 illustrates the difference between the foci achieved by the transmission matrix inversion method and the phase conjugation method for light focusing. In a given FOV (denoted by the red boxes in Fig. 1(a)), the transmission matrix inversion method has a higher PBR than that of the phase conjugation method, because the background can theoretically be suppressed to zero. For locations outside the FOV, the background intensity for both methods

are similar. Energy conservation is still satisfied because we only re-distribute the energy so as to improve the contrast inside the FOV, but not break the unitarity of the total transmission matrix.



Fig. 1. Illustration of focusing light to a target location by (a) the transmission matrix inversion method, and (b) the phase conjugation method. The red box in (a) denotes the selected field of view.

Simulation results are shown in Fig. 2. We generated a transmission matrix with a dimension of 49×100 , and used both the phase conjugation and the transmission matrix inversion methods to focus light to a single mode inside a FOV of 49 optical modes. The PBR of the focus achieved by the phase conjugation method (Fig. 2(a)) is ~ 51 . In comparison, the PBR of the focus achieved by the transmission matrix inversion method reaches infinity, since the background within the FOV is suppressed to zero (Fig. 2(b)). From Fig. 2, it can be seen that the tradeoff of our matrix inversion method is that the peak intensity is lower than that of the phase conjugation method, because some degrees of freedom are assigned to suppress the background.

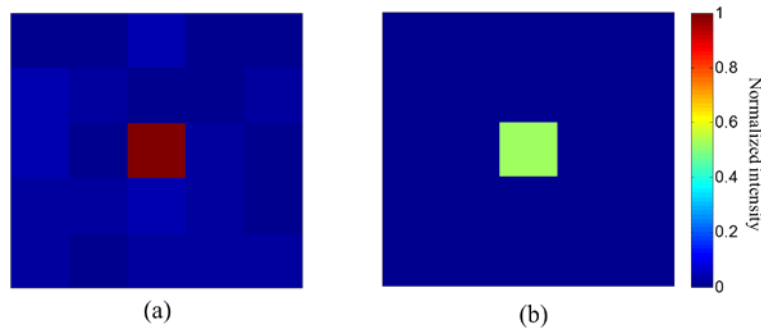


Fig. 2. Two-dimensional simulations of focusing light through a scattering medium to a target location by (a) phase conjugation, and (b) transmission matrix inversion.

In practice, the noise in the measurement of transmission matrix reduces the PBR, so the PBR cannot reach infinity. Based on the derivations in the Appendix, we theoretically prove that the PBR of the transmission matrix inversion method is determined by the ratio of the difference between the number of degrees of freedom to control light (n) and the number of modes in the FOV (m) to the normalized noise level (quantified by variance σ_n^2 , normalized by σ^2) in transmission matrix measurement:

$$\text{PBR} = \frac{n - m}{\sigma_n^2}. \quad (5)$$

If we fix n and rewrite Eq. (5), then $\text{PBR} = \frac{1-\beta}{\sigma_n^2} n$, where $\beta = \frac{m}{n}$. If $\frac{1-\beta}{\sigma_n^2} > 1$, PBR can be higher than n , which is the theoretical limit of the PBR in phase conjugation. Elaborations on Eq. (5) will be discussed in the Discussion section.

2.2 Focusing light to multiple target locations

Here, we demonstrate that our matrix inversion method enables light focusing to multiple foci with higher fidelity than those of conventional methods based on phase conjugation [15]. We use an example of focusing light to two target locations to explain the principle (Fig. 3). Since the phase conjugation method simply adds the fields of two focus light fields together (Fig. 3(a)), the peak of one focus interferes with the background associated with the other focus. Therefore, the peak intensity of the two foci is no longer equal due to the interference, even if they are equal when achieved individually by phase conjugation.

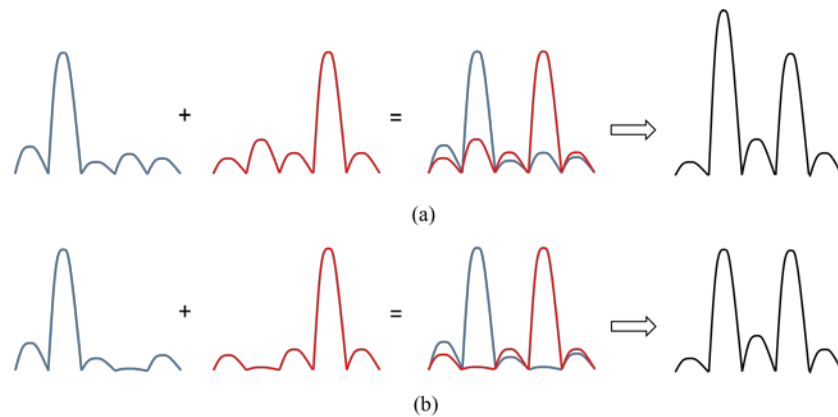


Fig. 3. Illustration of focusing light to two target locations by (a) phase conjugation and (b) transmission matrix inversion.

When the PBR of the focus is low, the amplitude of the peak is close to the amplitude of the background, so this low fidelity problem becomes even more severe for the phase conjugation method. In contrast, if we suppress the background associated with one focus at the position of the peak of the other focus, the peak intensities of the two foci would be equal (Fig. 3(b)). The matrix inversion method enables us to achieve this scheme. We first select the positions of the foci with equal focal light intensity, then at each focus position, the background associated with the other focus is automatically set to zero.

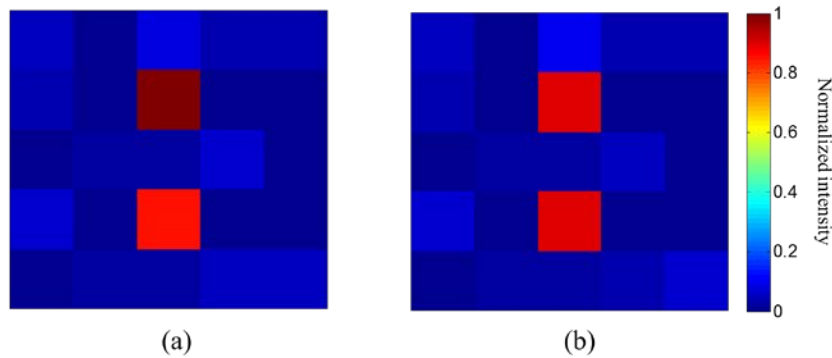


Fig. 4. Two-dimensional simulations of focusing light to two positions by (a) phase conjugation and (b) transmission matrix inversion.

Figure 4 shows the simulation results of focusing light to two locations through a scattering medium. The simulation parameters are the same as those used for focusing light to a single location. The intensities of the two foci achieved by phase conjugation are not equal (1 versus 0.86, see Fig. 4(a)), while the intensities of the two foci achieved by matrix inversion are equal (both are 0.9, see Fig. 4(b)). This result shows that the matrix inversion method achieves higher fidelity when focusing light to multiple locations. It should be noted that unlike controlling tens of optical modes in the single focus case shown in Fig. 2, here, we control only two optical modes at the two target foci locations. Therefore, the intensity of the foci achieved by matrix inversion is not sacrificed as much as that in the single focus case (Fig. 2).

3. Experiment

We experimentally demonstrate the aforementioned advantages of matrix inversion over phase conjugation to focus light through scattering media (Fig. 5). We first measured the transmission matrix of the scattering medium by on-axis four-step phase shifting holography [25]. A diode pumped laser (532 nm, 150 mW, CrystaLaser Inc. USA) was used as a light source. The polarization direction of the emitted light was rotated by a polarizer to make it align with the SLM operation direction. A beam splitter B1 split the light into two paths. The beam that passed through B1 was used as a reference beam for holography, and the beam reflected by B1 illuminated a phase-only-modulation SLM (PLUTO, HOLOEYE), which was relayed by lenses L1 and L2 onto a scattering medium made of ground glass (DG10-120, Thorlabs). A polarizer P blocked the light whose polarization was changed by the scattering medium. The scattered light then interfered with the reference beam on the camera sensor (GX1920, Allied Vision). By stepping the phases displayed on the SLM, we retrieved the scattered light field on the camera sensor. Since a portion of the light illuminated the SLM was not modulated, we used a 0th order block (a black disk with a diameter of 100 μm printed on a transparency) to eliminate this part of light. A phase gradient pattern was added on the SLM to prevent the modulated light from being blocked by the 0th order block. We chose 128 Hadamard bases as the incident fields, and for each Hadamard pattern we recorded the output field on the camera, which represented one column of the transmission matrix. After recording the transmission matrix, we blocked the reference beam by shutter S and used the transmission matrix inversion method to realize the desired focusing patterns.

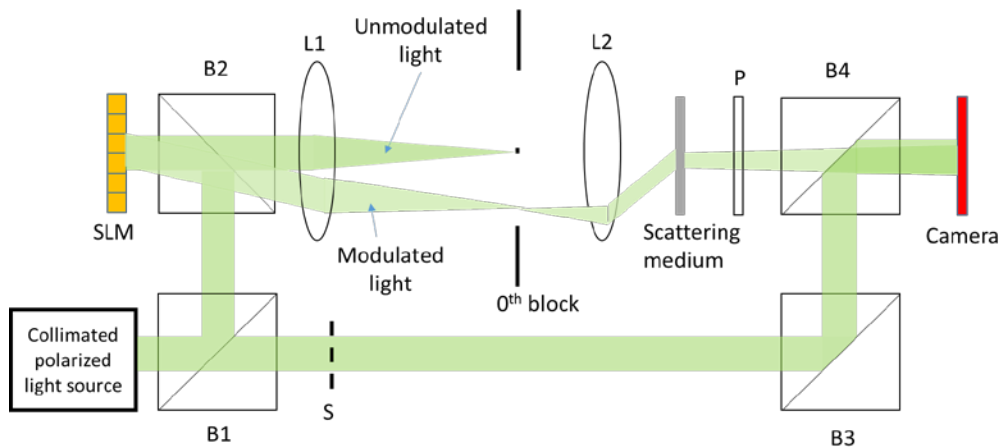


Fig. 5. Schematic of the experimental setup. B, beam splitter; L, lens; P, polarizer; S, shutter; SLM, spatial light modulator.

3.1 Focusing light to one target location with a higher PBR than phase conjugation

A workflow of focusing light to a target location with matrix inversion is shown in Fig. 6(a). To effectively suppress the background, we first used the conventional method – phase conjugation to realize one focus spot with a PBR of 21 (Figs. 6(b) and (d)). Then, we selected some bright background channels and performed matrix pseudoinversion. By doing this, we selectively darken the bright background speckle grains to improve the PBR to 35 (Figs. 6(c) and 6(e)), achieving a 66% improvement of PBR. The transmission matrix inversion method did not reduce the peak intensity much, but it suppressed the background around the focus. In our experiment, since we used a phase-modulation SLM, we simply took the phase of the calculated incident optical field while keeping the amplitude spatially uniform. We will discuss more about the impact of phase-only modulation in the Discussion section.

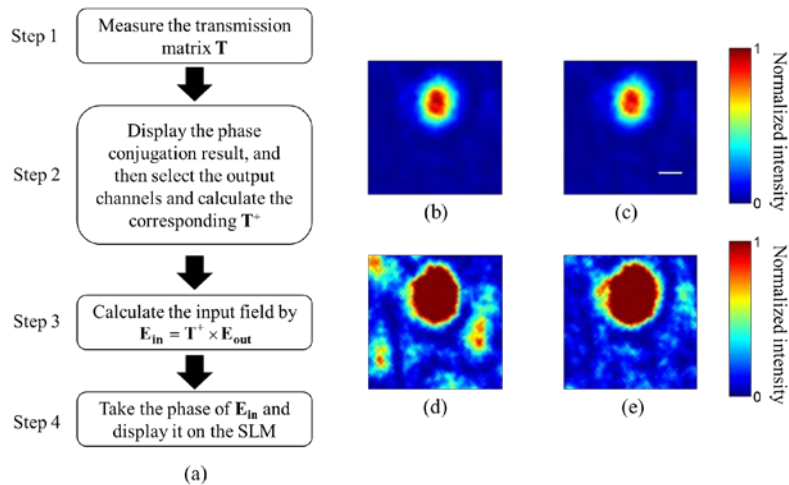


Fig. 6. (a) Workflow of realizing a high PBR focusing by matrix inversion. Optical focus achieved by (b) phase conjugation and (c) matrix inversion. Over-exposure images of the focus achieved by (d) phase conjugation and (e) matrix inversion to see the background speckle grains. Scale bar, 50 μm . $\beta = 0.1$ in our experiment.

3.2 Focusing light to multiple target locations with higher fidelity than phase conjugation

We demonstrate that matrix inversion enables a higher fidelity over phase conjugation when focusing light to multiple target locations in Fig. 7. Since the phase conjugation method simply adds different focus fields together (Section 2.2), the intensity of two foci is not equal, as shown in Figs. 7(a)-7(c). As the theory only considers the expected value of the output pattern, phase conjugation can only statistically guarantee that the intensity of the multiple foci are equal, so the focus intensity may not be equal when we only perform the experiment once. In contrast, the intensity of the multiple foci achieved by matrix inversion is more even (Figs. 7(d)-7(f)), because here the solution is exactly for realizing two focus spots with equal intensity. Therefore the deviation between the expected value and the one-time-realization in the phase conjugation method does not exist here. The patterns in Fig. 7 are captured based on three different transmission matrices since we move the scattering medium and the camera to show generality. The line profile comparisons between the foci achieved by the phase conjugation and the matrix inversion methods are shown in Figs. 7(g)-7(i).

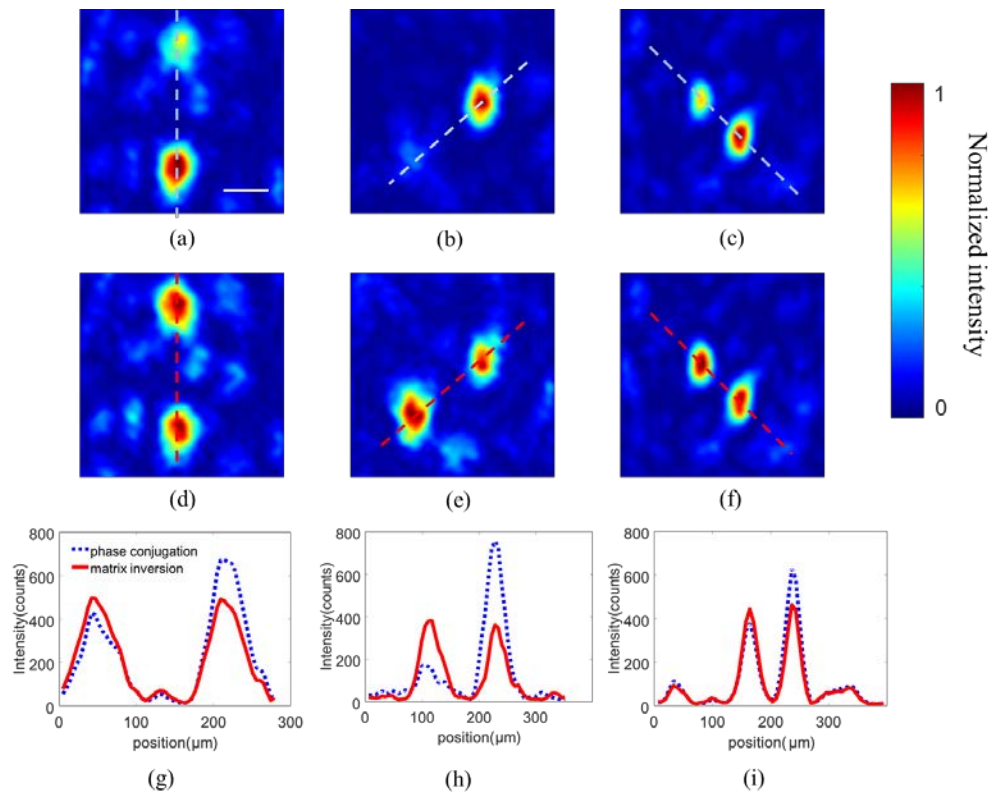


Fig. 7. Focusing light to two target locations achieved by phase conjugation ((a) – (c)) and by matrix inversion ((d) – (f)). (g) – (i) Line profiles of the foci shown in (a) – (f) achieved by phase conjugation and matrix inversion. Scale bar, 50 μm .

4. Discussion

Accurately measuring the transmission matrix is very important for transmission matrix inversion based optical focusing. Because of the measurement noises caused by air turbulence, photon shot noise, mechanical drift of the optical system, etc., the measured transmission matrix always deviates from the true transmission matrix. This deviation limits the PRB improvement of the transmission matrix inversion method. As shown in Eq. (5), if

we fix n , we have $\text{PBR} = \frac{n-m}{\sigma_n^2} = \frac{1-\beta}{\sigma_n^2}n$, where $\beta = \frac{m}{n}$. Simulation results match well with the theoretical results based on Eq. (5) (see Fig. 8). It is understandable that the PBR drops as β increases (Fig. 8(a)), since in this case we use limited degrees of freedom to control more output optical modes. Obviously, larger measurement errors in transmission matrix measurement lead to lower PBRs, as shown in Fig. 8 (b). For a given field of view (given β), when the noise level σ_n^2 is lower than $1-\beta$, the PBR can be higher than n . In this case, the PBR achieved by matrix inversion is higher than that achieved by phase conjugation.

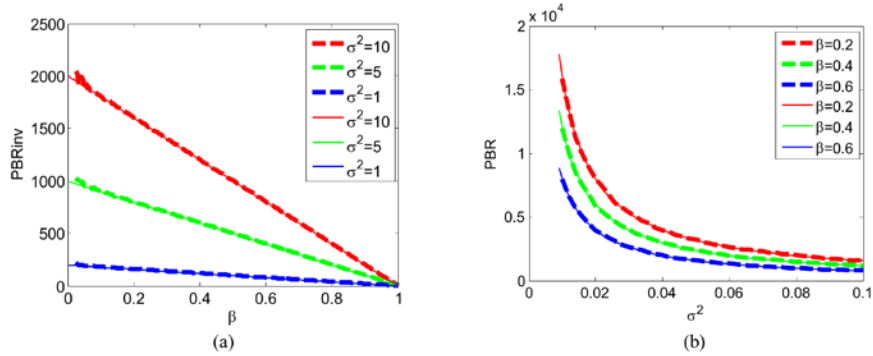


Fig. 8. PBR versus (a) β and (b) σ^2 as n is fixed as 200. Solid lines: theoretical calculation. Dashed lines: numerical simulations.

In our experiments described in Section 3, we applied phase-only modulation to realize the transmission matrix inversion method. Phase-only modulation can be treated as noisy amplitude-and-phase modulation since the amplitude of the modulated light deviates from the field calculated from the matrix inversion. However, phase-only modulation based matrix inversion method still outperforms phase-only modulation based phase conjugation when β is less than ~ 0.4 given the noise level in our experiment. Our experimental results match well with the numerical simulation results (see Fig. 9), where we set the normalized measurement noise σ_n as 1. Under this condition, we found that the difference between the PBRs of phase-only modulation and amplitude & phase modulation is about 60%.

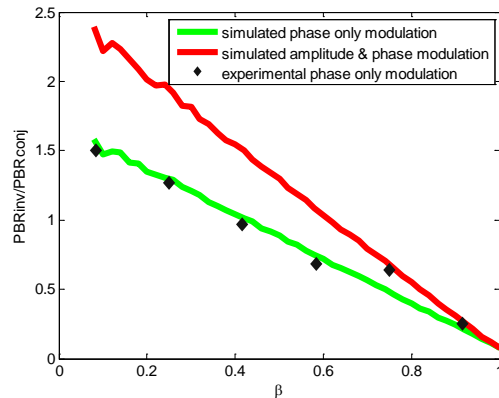


Fig. 9. Experimental and simulated ratios between the PBRs achieved by matrix inversion and phase conjugation, considering noise and phase-only modulation (black dots and green curve, respectively). Red curve shows the simulation result considering amplitude & phase modulation. In the simulation, $n = 128$ and $\sigma_n = 1$.

In addition to focusing, in a broader view, the transmission matrix inversion method can project a light pattern through scattering media. For example, the matrix inversion method can be used to darken a speckle field in a FOV without creating any focal spots like that demonstrated in Section 3, while phase conjugation cannot achieve this. In Section 3.1, if the target focus position is outside the FOV, what we see inside the FOV is that those bright speckle grains are darkened. Based on this principle, we can find the wavefront solution to darken speckles in a FOV using the following protocol. After measuring the transmission matrix corresponding to the FOV, we only need to add an arbitrary row \mathbf{r} into the measured transmission matrix \mathbf{T} to make a new transmission matrix $\mathbf{T}_{new} = \begin{bmatrix} \mathbf{r} \\ \mathbf{T} \end{bmatrix}$ and calculate its pseudoinverse $\mathbf{T}_{new}^+ = [\mathbf{c}_1 \ \mathbf{c}_2 \ \dots \ \mathbf{c}_{m+1}]$, where \mathbf{c}_i is the i^{th} column of \mathbf{T}_{new}^+ . Since $\mathbf{T}_{new} \times \mathbf{T}_{new}^+ = \mathbf{I}$, we get $\mathbf{T}_{new} \times \mathbf{c}_1 = [1 \ 0 \ \dots \ 0]^T$, which means that the first column \mathbf{c}_1 of \mathbf{T}_{new}^+ is orthogonal to all the rows of \mathbf{T} . Therefore, \mathbf{c}_1 is the wavefront solution to darken the speckle grains in the FOV. The experimental results are shown in Fig. 10, where we darkened the speckle grains in red circles in Figs. 10(d)-10(f) while keeping the speckle grains outside the FOV highly correlated with the original fields (Figs. 10(a)-10(c)). To show the generality of the method, we moved the camera and the diffuser at three different positions. Unlike the case with the matrix inversion method, the speckle grains in the red circles cannot be fully darkened by using the phase conjugation method, because if we replace the \mathbf{T}_{new}^+ above by $\mathbf{T}_{new}^* = [\mathbf{r}^* \ \mathbf{T}^*]$, there is no guarantee that the first column \mathbf{r}^* of \mathbf{T}_{new}^* is orthogonal to all the rows of \mathbf{T} .

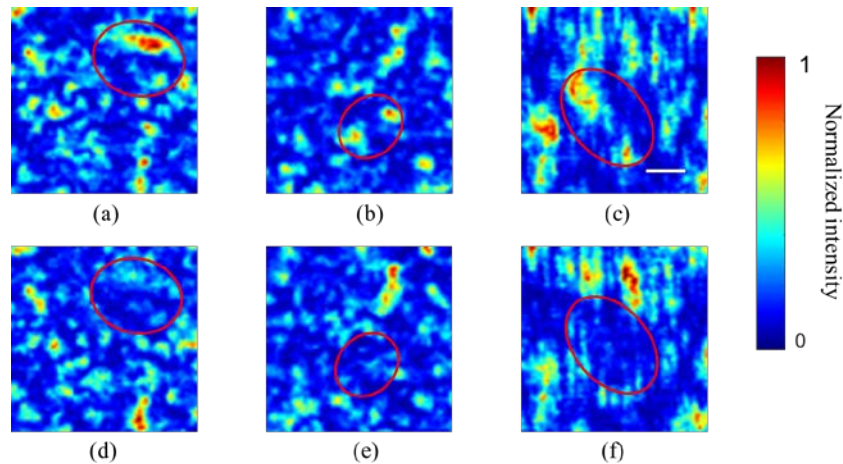


Fig. 10. Results of speckle darkening. The original speckle patterns before darkening are shown in (a) – (c). After using the matrix inversion method, we can selectively darken the speckle grains enclosed in the red circles ((d) – (f)). Scale bar, 50 μm .

5. Summary

In summary, we develop a transmission matrix inversion method for focusing light and projecting patterns through scattering media. We first theoretically and numerically prove the feasibility of this method, and then experimentally demonstrate that it can perform better than conventional methods under low noise conditions. By using this method, we obtain a higher PBR than that achieved by conventional methods in a given field of view. Moreover, our method improves the fidelity of focusing light to multiple locations through scattering media. This method can also be used for speckle darkening. We derive the analytical expression of the PBR achieved by our method, and predict that the performance can be improved if there

are methods to measure the transmission matrix more accurately or devices with known transmission matrices. Since high-contrast (high-PBR) and high-fidelity focusing is critical to many applications such as photolithography and confocal/two-photon microscopy, we believe our method will have an impact in these areas.

Appendix - Derivation of PBR

In the Appendix, all the letters in bold mean matrices, and the corresponding lowercase italic letters mean the elements in the matrices. Without losing generality, let us assume the desired output field as $[1 \ 0 \ \dots \ 0]^T$, then

$$\mathbf{E}_{\text{out}}^{\text{inv}} = \mathbf{T}_0 \times \mathbf{E}_{\text{in}}^{\text{inv}} = \mathbf{T}_0 \times (\mathbf{T}_0 + \mathbf{e})^+ \times \begin{bmatrix} 1 \\ 0 \\ \dots \\ 0 \end{bmatrix}, \quad (6)$$

where \mathbf{e} is the noise in transmission matrix measurement, thus $\mathbf{T}_0 \times (\mathbf{T}_0 + \mathbf{e})^+$ is no longer equal to \mathbf{I} . Here, $t_{ij} \sim CN(0,1)$, and we assume $e_{ij} \sim CN(0, \sigma_n^2)$. $\mathbf{T}_0 \times (\mathbf{T}_0 + \mathbf{e})^+$ can be rewritten as

$$\mathbf{T}_0 \times (\mathbf{T}_0 + \mathbf{e})^+ = \mathbf{I} - \mathbf{e}(\mathbf{T}_0 + \mathbf{e})^+. \quad (7)$$

While the first term, \mathbf{I} , in Eq. (7) multiplied by the desired output vector results in the peak intensity of the output, the second term leads to the background of the output field.

We then conduct singular value decomposition (SVD) [26] for $(\mathbf{T}_0 + \mathbf{e})$, that is $\mathbf{T}_0 + \mathbf{e} = \mathbf{UDV}^*$. By substituting it into Eq. (7), we have

$$\mathbf{I} - \mathbf{e}(\mathbf{T}_0 + \mathbf{e})^+ = \mathbf{I} - \mathbf{e}(\mathbf{UDV}^*)^+ = \mathbf{I} - \mathbf{eVD}^{-1}\mathbf{U}^* = \mathbf{I} - \tilde{\mathbf{e}}\mathbf{D}^{-1}\mathbf{U}^*. \quad (8)$$

Since \mathbf{V} is a unitary matrix, thus $\tilde{\mathbf{e}} = \mathbf{eV}$ is still a complex random Gaussian matrix with the same distribution as \mathbf{e} [27]. The background of $\mathbf{E}_{\text{out}}^{\text{inv}}$ is equal to the mean value of the square of the norm (\bar{l}_2) of the element b_{ij} in $\mathbf{b} = \tilde{\mathbf{e}}\mathbf{D}^{-1}\mathbf{U}^*$. Because unitary matrix \mathbf{U}^* does not change the \bar{l}_2 of b_{ij} , we only need to calculate the \bar{l}_2 of b'_{ij} in $\mathbf{b}' = \tilde{\mathbf{e}}\mathbf{D}^{-1} = \tilde{\mathbf{e}}\mathbf{\Gamma}$. Thus the \bar{l}_2 of b'_{ij} is

$$\langle |b'_{ij}|^2 \rangle = \left\langle \frac{1}{m^2} \left| \sum_{j=1}^m \sum_{i=1}^m \tilde{e}_{ij} \gamma_{ii} \right|^2 \right\rangle = \left\langle \frac{1}{m} \left| \sum_{i=1}^m \tilde{e}_{ij} \gamma_{ii} \right|^2 \right\rangle = \langle |\tilde{e}_{ij}|^2 \gamma_{ii}^2 \rangle. \quad (9)$$

Here, $\langle |b'_{ij}|^2 \rangle$ means the ensemble average of $|b'_{ij}|^2$. If we assume \mathbf{e} and $(\mathbf{T}_0 + \mathbf{e})$ are independent (this approximation holds if $\sigma_n^2 \ll 1$). Numerical results show that this approximation still works well when $\sigma_n^2 \sim 1$), $\tilde{\mathbf{e}}$ and $\mathbf{\Gamma}$ are also independent. In this case, Eq. (9) becomes

$$\langle |b'_{ij}|^2 \rangle = \langle |\tilde{e}_{ij}|^2 \gamma_{ii}^2 \rangle = \langle |\tilde{e}_{ij}|^2 \rangle \langle \gamma_{ii}^2 \rangle = 2\sigma_n^2 \langle \gamma_{ii}^2 \rangle. \quad (10)$$

Random matrix theories show that the probability density function (PDF) of singular value d of a m by n standard complex Gaussian matrix is [27]

$$p_d(x) = \frac{\sqrt{-\left(\frac{x^2}{2n} - (1 + \sqrt{\beta})^2\right)\left(\frac{x^2}{2n} - (1 - \sqrt{\beta})^2\right)}}{\pi\beta x}, \beta = \frac{m}{n} < 1. \quad (11)$$

Since $\gamma_{ii}^2 = d_{ii}^{-2}$, we have the PDF of γ_{ii}^2

$$p_{\gamma^2}(y) = \frac{\sqrt{-\left(\frac{1}{2ny} - (1 + \sqrt{\beta})^2\right)\left(\frac{1}{2ny} - (1 - \sqrt{\beta})^2\right)}}{2\pi\beta y}, \beta = \frac{m}{n} < 1. \quad (12)$$

Therefore, we have $\langle \gamma_{ii}^2 \rangle = \int_{\frac{1-\sqrt{\beta}}{2n}}^{\frac{2n}{1+\sqrt{\beta}}}$ $y p_{\gamma^2}(y) dy = \frac{1}{2n(1-\beta)}$. Substituting it to Eq. (10), we get

$$\langle |b_{ij}|^2 \rangle = \frac{\sigma_n^2}{n(1-\beta)}. \quad (13)$$

Ensemble average of peak intensity $\langle |p_i|^2 \rangle = \langle |1 - b_{ii}|^2 \rangle = 1 + \langle |b_{ii}|^2 \rangle = 1 + \frac{\sigma_n^2}{n(1-\beta)}$. Finally, we have

$$PBR = \frac{\langle |p_i|^2 \rangle}{\langle |b_{ij}|^2 \rangle} = \frac{n-m}{\sigma_n^2} + 1 \approx \frac{n-m}{\sigma_n^2}. \quad (14)$$

Funding

National Institutes of Health (NIH 1U01NS090577); GIST-Caltech Collaborative Research (CG2016).

Acknowledgments

The authors would like to thank Dr. Anatoly Khina and Peida Tian for helpful discussions.